Inorg. Chem. **2004**, *43*, 6083–6092

Room Temperature Phosphorescence from Ruthenium(II) Complexes Bearing Conjugated Pyrenylethynylene Subunits

Denis V. Kozlov,[§] Daniel S. Tyson,[§,¶] Christine Goze,[‡] Raymond Ziessel,*[,‡] and Felix N. Castellano*[,§]

Laboratoire de Chimie Moléculaire, ECPM, 25 rue Becquerel, 67087 Strasbourg Cedex 02, France, and Department of Chemistry and Center for Photochemical Sciences, Bowling Green State University, Bowling Green, Ohio 43403

Received June 1, 2004

We describe the synthesis, electrochemistry, and photophysical properties of several Ru(II) complexes bearing different numbers of pyrenylethynylene substituents in either the 5- or 5,5′-positions of 2,2′-bipyridine, along with the appropriate Ru(II) model complexes bearing either bromo- or ethynyltoluene functionalities. In addition, we prepared and studied the photophysical behavior of the diimine ligands 5-pyrenylethynylene-2,2′-bipyridine and 5,5′-dipyrenylethynylene-2,2′-bipyridine. Static and dynamic absorption and luminescence measurements reveal the nature of the lowest excited states in each molecule. All model Ru(II) complexes are photoluminescent at room temperature and exhibit excited-state behavior consistent with metal-to-ligand charge transfer (MLCT) characteristics. In the three Ru(II) molecules bearing multiple pyrenylethynylene substituents, there is clear evidence that the lowest excited state is triplet intraligand (^{3}IL)-based, yielding long-lived room temperature phosphorescence in the red and near IR. This phosphorescence emanates from either 5-pyrenylethynylene-2,2′-bipyridine or 5,5′-dipyrenylethynylene-2,2′-bipyridine, depending upon the composition of the coordination compound. In the former case, the excited-state absorption difference spectra that were measured for the free ligand are easily superimposed with those obtained for the metal complexes coordinated to either one or two of these species. The latter instance is slightly complicated since coordination of the 5,5′-ligand to the Ru(II) center planarizes the diimine structure, leading to an extended conjugation on the long axis with a concomitant red shift of the singlet π–π^* absorption transitions and the observed room temperature phosphorescence. As a result, transient absorption measurements obtained using free 5,5′-dipyrenylethynylene-2,2′-bipyridine show a marked blue shift relative to its Ru(II) complex, and this extended π-conjugation effect was confirmed by coordinating this ligand to Zn(II) at room temperature. In essence, all three pyrenylethynylene-containing Ru(II) complexes are unique in this genre of chromophores since the lowest excited state is ^{3}IL-based at room temperature and at 77 K, and there is no compelling evidence of interacting or equilibrated excited states.

Introduction

The introduction of selected organic chromophores into diimine ligand structures has generated a wide variety of inorganic complexes with novel photophysical properties.[1−19] Particularly noteworthy are those complexes which display low-lying metal-to-ligand charge transfer (MLCT) excited states whose triplet levels are coincident with those of the

* Authors to whom correspondence should be addressed. E-mail: ziessel@chimie.u-strasbg.fr (R.Z.); castell@bgnet.bgsu.edu (F.N.C.).
§ Bowling Green State University.
‡ ECPM.
¶ Current address: Ohio Aerospace Institute and NASA Glenn Research Center, 22800 Cedar Point Road, Cleveland, OH 44142.

(1) Wang, X.-Y.; Del Guerzo, A.; Schmehl, R. H. *J. Photochem. Photobiol., C* **2004**, *5*, 55−77.
(2) Ford, W. E.; Rodgers, M. A. J. *J. Phys. Chem.* **1992**, *96*, 2917−2920.
(3) Wilson, G. J.; Launikonis, A.; Sasse, W. H. F.; Mau, A. W. H. *J. Phys. Chem. A* **1997**, *101*, 4860−4866.
(4) Simon, J. A.; Curry, S. L.; Schmehl, R. H.; Schatz, T. R.; Piotrowiak, P.; Jin, X.; Thummel, R. P. *J. Am. Chem. Soc.* **1997**, *119*, 11012−11022.
(5) Tyson, D. S.; Castellano, F. N. *J. Phys. Chem. A* **1999**, *103*, 10955−10960.
(6) Tyson, D. S.; Bialecki, J.; Castellano, F. N. *Chem. Commun.* **2000**, 2355−2356.
(7) Tyson, D. S.; Henbest, K. B.; Bialecki, J.; Castellano, F. N. *J. Phys. Chem. A* **2001**, *105*, 8154−8161.
(8) Tyson, D. S.; Luman, C. R.; Zhou, X.; Castellano, F. N. *Inorg. Chem.* **2001**, *40*, 4063−4071.

10.1021/ic049288+ CCC: $27.50
Published on Web 08/26/2004

covalently linked organic system(s). Such metal−organic chromophores have generated room temperature (RT) excited-state lifetimes in excess of 100 μs, which radiatively decay through the MLCT manifold. In cases where the metal center is ruthenium(II), most of the documented behavior can be explained by the excited-state equilibrium or the slow back energy transfer processes between ^{3}MLCT and intraligand (^{3}IL) excited states. An alternative approach in generating long lifetime RT emission is to select a diimine ligand system whose ^{3}IL states are substantially lower in energy relative to the ^{3}MLCT level. Here, singlet MLCT excitation can lead to rapid intersystem crossing and the observation of either pure ^{3}IL or mixed ^{3}IL/intraligand charge transfer (^{3}ILCT) phosphorescence at RT.[13−17,20] In a recent report, our groups demonstrated that RT phosphorescence can also be generated in Pt(II) diimine bis(acetylide) chromophores, where the ^{3}IL excited states are remote from the diimine ligand structure.[21]

A fundamental issue in this area concerns the "transitioning" of photophysics in molecules where either MLCT or IL excited states dominate the behavior. For example, small structural modifications that alter the energy of the MLCT and/or the IL states can completely transform the observed photophysics toward either extreme. The Ziessel and Schanze groups have very recently illustrated this transitional behavior in structurally related oligo(thiophene-bipyridine)-containing Ru(II) complexes.[16,17] Compelling evidence was presented for one of their polynuclear complexes where the photophysics could best be described as a composite of MLCT and IL behavior, somewhat between that expected for each.[17] At the present time, this effect may be explained by a thermal excited-state equilibrium or by configuration mixing. Solvent medium has also been used to influence and mediate the excited-state processes in transition-metal complexes possessing multiple chromophores.[22,23] In one example, triplet energy transfer was turned "on" and "off" by varying the solvent in a Ru(II)−cyanide complex.[22] In another system, solvent polarity transitioned the photophysical behavior from predominately ^{3}MLCT to ^{3}IL in a multichromophoric Pt(II) complex.[23] Undoubtedly, there is a wealth of excited-state behavior that remains to be explored in the realm of metal−organic chromophores and assemblies.

Scheme 1 [a]

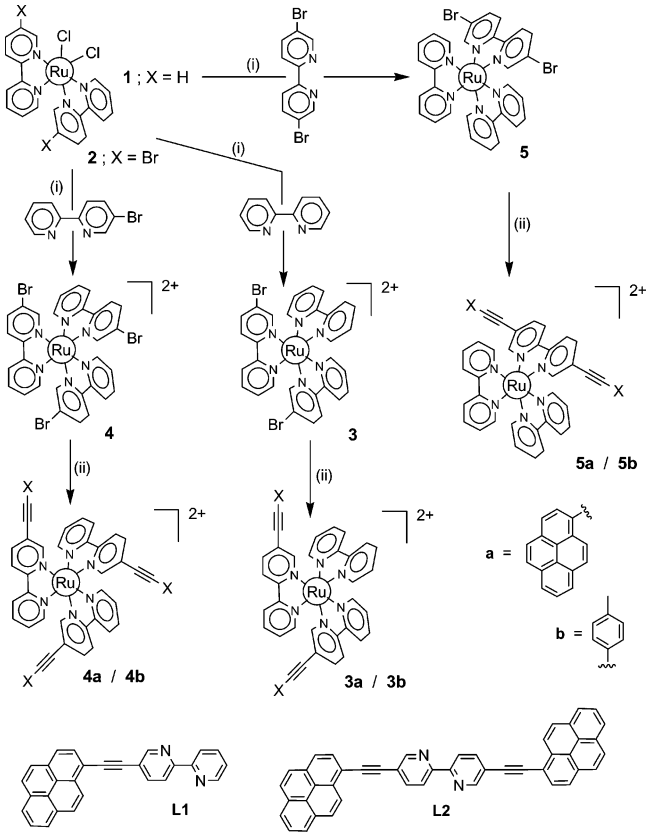

[a] (i) 6:1 (v/v) EtOH/H_2O, 80 °C; (ii) 6 mol % [$Pd(PPh_3)_4$], 1:1 (v/v) CH_3CN/benzene, iPr$_2$NH. All counteranions are PF_6^-.

In the current paper, we report the synthesis and photophysical properties of a series of ruthenium(II) diimine chromophores that contain different numbers of pyrenylethynylene substituents in either the 5- or 5,5′-positions of 2,2′-bipyridine (bpy) (**3a**, **4a**, and **5a** in Scheme 1). Since the pyrenylethynyl linkages are directly conjugated to the bipyridine ligands, this study represents a departure from our previous work on Ru(II) systems where the organic chomophore(s) could be viewed independently from the metal complex. We have measured the static and dynamic absorption and photoluminescence properties of these molecules along with the model systems containing the appropriate Br or ethynyltoluene substituents and the "free" pyrenyl-containing ligands. On the basis of the photophysical data, all of the molecules containing the Br or ethynyltoluene substituents display characteristic dπ(Ru) → π*(L) MLCT excited states (where L is the 5- or 5,5′-substituted bipyridine ligand(s)), whereas the molecules bearing the pyrenyl unit(s) are dominated by ^{3}IL excited states (within L) exhibiting room temperature phosphorescence. The combination of the ethynylene linkage with the 5- or 5,5′-substitution pattern leads to low-lying ^{3}IL excited states, distinct from all previously reported pyrenyl-containing Ru(II) complexes.

(9) Harriman, A.; Hissler, M.; Khatyr, A.; Ziessel, R. *Chem. Commun.* **1999**, 735−736.
(10) Hissler, M.; Harriman, A.; Khatyr, A.; Ziessel, R. *Chem.*−*Eur. J.* **1999**, *11*, 3366−3381.
(11) McClenaghan, N. D.; Barigelletti, F.; Maubert, B.; Campagna, S. *Chem. Commun.* **2002**, 602−603.
(12) Maubert, B.; McClenaghan, N. D.; Indelli, M. T.; Campagna, S. *J. Phys. Chem. A* **2003**, *107*, 447−455.
(13) Michalec, J. F.; Bejune, S. A.; McMillin, D. R. *Inorg. Chem.* **2000**, *39*, 2708−2709.
(14) Del Guerzo, A.; Leroy, S.; Fages, F.; Schmehl, R. H. *Inorg. Chem.* **2002**, *41*, 359−366.
(15) Shaw, J. R.; Schmehl, R. H. *J. Am. Chem. Soc.* **1991**, *113*, 389−394.
(16) De Nicola, A.; Liu, Y.; Schanze, K. S.; Ziessel, R. *Chem. Commun.* **2003**, 288−289.
(17) Liu, Y.; De Nicola, A.; Reiff, O.; Ziessel, R.; Schanze, K. S. *J. Phys. Chem. A* **2003**, *107*, 3476−3485.
(18) Ley, K. D.; Schanze, K. S. *Coord. Chem. Rev.* **1998**, *171*, 287−307.
(19) Walters, K. A.; Ley, K. D.; Cavalaheiro, C. S. P.; Miller, S. E.; Gosztola, D.; Wasielewski, M. R.; Bussandri, A. P.; van Willigen, H.; Schanze, K. S. *J. Am. Chem. Soc.* **2001**, *123*, 8329−8342.
(20) Watts, R. J.; Crosby, G. A.; Sansregret, J. L. *Inorg. Chem.* **1972**, *11*, 1474−1483.
(21) Pomestchenko, I. E.; Luman, C. R.; Hissler, M.; Ziessel, R.; Castellano, F. N. *Inorg. Chem.* **2003**, *42*, 1394−1396.
(22) Indelli, M. T.; Ghirotti, M.; Prodi, A.; Chiorboli, C.; Scandola, F.; McClenaghan, N. D.; Puntoriero, F.; Campagna, S. *Inorg. Chem.* **2003**, *42*, 5489−5497.
(23) Pomestchenko, I. E.; Castellano, F. N. *J. Phys. Chem. A* **2004**, *108*, 3485−3492.

In essence, the conjugated ligand structures render the ^{3}IL states so low in energy, relative to the MLCT states, that no significant electronic interactions can be readily observed. We note that some preliminary accounts of this work have already been disseminated.[24,25]

Experimental Section

General. 1-Bromopyrene, 2,2′-bipyridine (bpy), zinc(II) acetate, and thioxanthone were obtained from commercial sources and used without further purification. 5-Bromo-2,2′-bipyridine, 1-trimethylsilylethynylpyrene, 1-ethynylpyrene, 5-(1-ethynylpyrene)-2,2′-bipyridine,[10] and *cis*-$[Ru(bpy)_2Cl_2]\cdot 2H_2O$[26] were prepared according to literature procedures. Diisopropylamine was dried over suitable reagents and distilled under argon immediately prior to use. The ^{1}H and ^{13}C spectra were recorded at room temperature on a Bruker AC 200 MHz, a Bruker Avance 400 MHz, or on a Bruker Avance 300 MHz spectrometer, unless otherwise specified, using perdeuterated solvents with residual protonated solvents serving as internal standards (for ^{1}H spectra, $\delta = 7.26$ ppm for $CDCl_3$ and $\delta = 5.32$ ppm for CD_2Cl_2; for ^{13}C spectra, $\delta = 77.0$ ppm for $CDCl_3$ and $\delta = 53.8$ ppm for CD_2Cl_2). All carbon signals were detected as singlets. Fast atom bombardment (FAB, positive mode) mass spectra were recorded with a ZAB−HF−VB analytical apparatus with *m*-nitrobenzyl alcohol (*m*-NBA) as the matrix. Electrospray mass spectra (ES-MS) were recorded on a 1100 MSD Hewlett-Packard spectrometer. FT-IR spectra were recorded as KBr pellets.

Syntheses. Ruthenium(II)(5-bromo-2,2′-bipyridine)$_2$-dichloride (2). 5-Bromo-2,2′-bipyridine (0.500 g, 2 mmol) was added to a stirred solution of $RuCl_3\cdot 6H_2O$ (0.205 g, 0.98 mmol) in 20 mL of DMF with 0.200 g of LiCl. After the solution was heated for 8 h, the solvent was removed under vacuum and the crude product was precipitated in dichloromethane/hexane. The precipitate was washed with two portions of water (10 mL) and two portions of diethyl ether (10 mL) and dried to yield 0.330 g (50%) of product. Anal. Calcd for $C_{20}H_{12}Br_2Cl_2N_4Ru$: C, 37.53; H, 1.89; N, 8.75. Found: C, 37.17; H, 1.92; N, 8.59.

General Procedure 1 for the Preparation of the Bromo-Substituted Ruthenium(II) Complexes. In a Schlenk flask, to a stirred ethanol solution of the precursor complex was added the polypyridine ligand. The mixture was heated for 16 h at 80 °C until the complete consumption of the starting material was observed. After the solution cooled to room temperature, the solution was filtered, potassium hexafluorophosphate in water was added, and the solution was evaporated. The crude precipitate was washed two times with water and one time with diethyl ether and was chromatographed. The fractions containing the pure complex were evaporated to dryness and recrystallized by the slow evaporation of CH_2Cl_2 from a mixture of CH_2Cl_2/hexanes, approximately 80/20 (v/v).

[Ruthenium(II)(2,2′-bipyridine)$_2$(5,5′-dibromo-2,2′-bipyridine)]-(PF$_6$)$_2$ (5). Complex **5** was prepared according to general procedure 1 with 100 mg of *cis*-$[Ru(bpy)_2Cl_2]$ (0.19 mmol), 60 mg of 5,5′-dibromo-2,2′-bipyridine (0.19 mmol), and 20 mL of ethanol. The crude product was purified by chromatography on a column packed with alumina and eluting with a gradient of methanol in dichloromethane from 0 to 2%. Recrystallization gave 98 mg (55%) of analytically pure product. ^{1}H NMR ($CDCl_3$, 200 MHz): δ 8.49 (m, 4H), 8.38 (d, 2H, $^3J = 8.8$ Hz), 8.23 (dd, 2H, $^3J = 8.8$ Hz, $^4J = 2.1$ Hz), 8.07 (m, 4H), 7.75 (d, 2H, $^3J = 5.5$ Hz), 7.73 (d, 2H, $^4J = 2.1$ Hz), 7.65 (d, 2H, $^3J = 5.1$ Hz), 7.41 (m, 4H). ^{13}C{^{1}H} NMR (CD_3CN, 300 MHz): δ 157.9, 157.8, 156.3, 153.3, 153.1, 152.7, 141.6, 139.10, 139.09, 128.6, 128.5, 126.2, 125.4, 125.3, 124.5. FT-IR (KBr, cm^{-1}): υ 2962 (m), 2918 (m), 2851 (m), 1619 (m), 1603 (s), 1458 (s), 1446 (s), 1261 (s), 1105 (m), 1083 (s), 1036 (m), 840 (s), 766 (m), 728 (m), 557 (s). UV−vis (CH_3CN) λ, nm (ϵ, M^{-1} cm^{-1}): 448 (11 000), 287 (61 500), 255 (22 200). FAB$^+$ (CH_3CN): 872.2 ($[M - PF_6]^+$). Anal. Calcd for $C_{30}H_{22}Br_2F_{12}N_6P_2Ru$: C, 35.42; H, 2.18; N, 8.26. Found: C, 35.29; H, 1.97; N, 8.04.

[Ruthenium(II)(2,2′-bipyridine)(5-bromo-2,2′-bipyridine)$_2$]-(PF$_6$)$_2$ (3). Complex **3** was prepared according to general procedure 1 with 150 mg of **2** (0.22 mmol), 34.5 mg of 2,2′-bipyridine (1 equiv, 0.22 mmol), and 30 mL of ethanol and 10 mL of water. The crude product was purified by chromatography on a column packed with alumina and eluting with a gradient of methanol in dichloromethane from 0 to 5%. Recrystallization gave 163 mg (73%) of analytically pure product. FT-IR (KBr, cm^{-1}): υ 3445 (m), 2919 (m), 1619 (m), 1460 (s), 1435 (s), 1261 (m), 1198 (m), 840 (s), 795 (m), 765 (m), 740 (m), 557 (s). UV−vis (CH_3CN) λ, nm (ϵ, M^{-1} cm^{-1}): 450 (12 100), 292 (70 300), 255 (24 400). ES-MS (CH_3CN): 872.2 ($[M - PF_6]^+$). Anal. Calcd for $C_{66}H_{40}F_{12}N_6P_2Ru$: C, 35.42; H, 2.18; N, 8.26. Found: C, 35.52; H, 2.33; N, 8.44.

[Ruthenium(II)(5-dibromo-2,2′-bipyridine)$_3$](PF$_6$)$_2$ (4). Complex **4** was prepared according to general procedure 1 with 150 mg of **2** (0.22 mmol), 56 mg of 5-bromo-2,2′-bipyridine (1 equiv, 0.22 mmol), and 30 mL of ethanol and 10 mL of water. The crude product was purified by chromatography on a column packed with alumina and eluting with a gradient of methanol in dichloromethane from 0 to 10%. Recrystallization gave 98 mg (41%) of analytically pure product. FT-IR (KBr, cm^{-1}): υ 3400 (m), 2928 (m), 1738 (m), 1603 (m), 1459 (s), 1435 (s), 1384 (m), 1369 (m), 1234 (m), 1082 (s), 840 (s), 782 (m), 752 (m), 557 (s). UV−vis (CH_3CN) λ, nm (ϵ, M^{-1} cm^{-1}): 450 (11 900), 294 (73 400), 265 (29 400). ES-MS (CH_3CN): 950.8 ($[M - PF_6]^+$), 403.5 ($[M - 2PF_6]^{2+}$). Anal. Calcd for $C_{66}H_{40}F_{12}N_6P_2Ru$: C, 32.87; H, 1.93; N, 7.67. Found: C, 32.95; H, 2.07; N, 7.81.

General Procedure 2 for the Preparation of the Ethynylpyrene- or Ethynyltoluyl-Substituted Ruthenium(II) Complexes. In a Schlenk flask, to a stirred degassed 50/50 acetonitrile/benzene solution of the precursor complex were added sequentially $Pd(PPh_3)_4$, diisopropylamine, and the acetylenic ligand. The mixture was heated under argon for 16 h until the complete consumption of the starting material was observed. After the solution cooled to room temperature, potassium hexafluorophosphate in water was added and the solution was evaporated. The crude precipitate was washed two times with water and one time with diethyl ether and was chromatographed. The fractions containing the pure complex were evaporated to dryness and recrystallized in CH_2Cl_2/hexane.

[Ruthenium(II)(2,2′-bipyridine)$_2$(5,5′-{1-ethynylpyrene})-2,2′-bipyridine](PF$_6$)$_2$ (5a). 5a was prepared according to general procedure 2 with 40 mg of **5** (0.035 mmol) in 2 mL of acetonitrile and 2 mL of benzene, 17 mg of 1-ethynylpyrene (2.15 equiv, 0.075 mmol), 2 mg of $[Pd(PPh_3)]$ (6% mol), and 1 mL of iPr$_2$NH. The chromatography was performed on a column packed with alumina and eluting with acetonitrile/toluene (80:20). Recrystallization in propionitrile/THF gave 43 mg of **5a** (69%). ^{1}H NMR (CD_3CN, 400 MHz): δ 8.62 (m, 4H), 8.47 (d, 2H, $^3J = 9.2$ Hz), 8.43 (d, 2H, $^3J = 7.3$ Hz), 8.39 (m, 4H), 8.33 (d, 2H, $^3J = 9.2$ Hz), 8.28 (d, 4H, $^3J = 8.9$ Hz), 8.17 (m, 10H), 8.12 (m, 2H), 8.04 (d, 2H, $^4J =$

(24) Goze, C.; Kozlov, D. V.; Castellano, F. N.; Suffert, J.; Ziessel, R. *Tetrahedron Lett.* **2003**, *44*, 8713−8716.
(25) Goze, C.; Kozlov, D. V.; Tyson, D. S.; Ziessel, R.; Castellano, F. N. *New J. Chem.* **2003**, *27*, 1679−1683.
(26) Sprintschnik, G.; Sprintschnik, H. W.; Kirsch, P. P.; Whitten, D. G. *J. Am. Chem. Soc.* **1977**, *99*, 4947−4954.

1.3 Hz), 7.98 (d, 2H, ^3J = 5.4 Hz), 7.86 (d, 2H, ^3J = 5.1 Hz), 7.54 (m, 4H). $^{13}C\{^1H\}$ NMR (CD_3CN, 400 MHz): δ 158.1, 158, 156.3, 154.6, 153.2, 153, 140.3, 139, 133.4, 133.1, 132.2, 131.8, 130.8, 130.2, 128.7, 128.6, 128.2, 127.9, 127.5, 127.4, 125.9, 125.6, 125.5, 125.4, 125.3, 125.1, 125, 124.7, 96.9 (C≡C), 90.9 (C≡C). FT-IR (KBr, cm^{-1}): υ 3437 (m), 2918 (m), 2851.6 (m), 2192 (C≡C) (m), 1619 (m), 1445 (s), 1261 (m), 1152 (m), 840 (s), 760 (m), 730 (m), 569 (m). UV−vis (CH_3CN) λ, nm (ϵ, M^{-1} cm^{-1}): 442 (29 000), 389 (20 000), 284 (60 000), 245 (45 000). FAB^+ (CH_3CN): 1163.4 ($[M - PF_6]^+$), 509.2 ($[M - 2PF_6]^{2+}$). Anal. Calcd for $C_{66}H_{40}F_{12}N_6P_2Ru$: C, 60.6; H, 3.08; N, 6.42. Found: C, 60.42; H, 2.87; N, 6.13.

[Ruthenium(II)(2,2′-bipyridine)(5-{1-ethynylpyrene}-2,2′-bipyridine)$_2$](PF$_6$)$_2$ (3a). 3a was prepared according to general procedure 2 with 70 mg of **3** (0.069 mmol) in 3 mL of acetonitrile and 3 mL of benzene, 39 mg of 1-ethynylpyrene (2.5 equiv, 0.17 mmol), 5 mg of [Pd(PPh_3)] (6% mol), and 1.5 mL of iPr$_2$NH. The chromatography was performed on a column packed with alumina and eluting with CH_3CN/toluene (60:40). Recrystallization gave 78 mg of **3a** (86%). FT-IR (KBr, cm^{-1}): υ 3400 (m), 2919 (m), 2853 (m), 2192 (C≡C) (s), 1623 (m), 1601 (s), 1464 (s), 1374 (m), 1240 (m), 1196 (m), 839 (s), 785 (m), 764 (m), 731 (m), 557 (s). UV−vis (CH_3CN) λ, nm (ϵ, M^{-1} cm^{-1}): 421 (39 000), 386 (36 300), 283 (58 000), 243 (58 200). ES-MS (CH_3CN): 1163.2 ($[M - PF_6]^+$), 509.3 ($[M - 2PF_6]^{2+}$). Anal. Calcd for $C_{66}H_{40}F_{12}N_6P_2Ru$: C, 60.6; H, 3.08; N, 6.42. Found: C, 60.4; H, 2.81; N, 6.17.

[Ruthenium(II)(5-{1-ethynylpyrene}-2,2′-bipyridine)$_3$](PF$_6$)$_2$ (4a). 4a was prepared according to general procedure 2 with 60 mg of **4** (0.069 mmol) in 3 mL of acetonitrile and 3 mL of benzene, 43.5 mg of 1-ethynylpyrene (3.5 equiv, 0.192 mmol), 3.8 mg of [Pd(PPh_3)] (6% mol), and 1.5 mL of iPr$_2$NH. The chromatography was performed on a column packed with alumina using CH_3CN/toluene (60:40) as eluent. Recrystallization gave 57 mg of **4a** (68%). FT-IR (KBr, cm^{-1}): υ 3368 (m), 2920 (m), 2853 (m), 2192 (C≡C) (s), 1623 (m), 1601 (s), 1464 (s), 1374 (m), 1240 (m), 1196 (m), 840 (s), 785 (m), 752 (m), 728 (m), 557 (s). UV−vis (CH_3CN) λ, nm (ϵ, M^{-1} cm^{-1}): 420 (72 400), 387 (69 000), 366 (54 500), 297 (91 000). ES-MS (CH_3CN): 1387.43 ($[M - PF_6]^+$), 621.19 ($[M - 2PF_6]^{2+}$), 1243.4 ($[M - 2PF_6 + H]^+$). Anal. Calcd for $C_{84}H_{48}F_{12}N_6P_2Ru$: C, 65.84; H, 3.16; N, 5.48. Found: C, 65.68; H, 2.93; N, 5.23.

[Ruthenium(II)(2,2′-bipyridine)$_2$(5,5′-{*p*-ethynyltoluene}-2,2′-bipyridine)](PF$_6$)$_2$ (5b). 5b was prepared according to general procedure 2 with 25 mg of **5** (0.049 mmol) in 1.5 mL of acetonitrile and 1.5 mL of benzene, 16 μL of *p*-ethynyltoluene (5 equiv, 0.105 mmol), 10.5 mg of [Pd(PPh_3)] (10% mol), and 0.5 mL of iPr$_2$NH. The crude product was purified by chromatography on a column packed with silica gel and eluting with an acetonitrile/water/aqueous saturated KNO_3 mixture (85:15:0 to 85:15:0.05). After anionic exchange, the analytically pure compound was obtained after recrystallization from dichloromethane/hexane (26 mg, 94%). ^1H NMR (CD_3CN, 300 MHz): δ 8.52 (m, 6H), 8.15 (dd, 2H, ^3J = 8.46 Hz, ^4J = 1.68 Hz), 8.10 (m, 4H), 7.84 (m, 4H), 7.72 (d, 2H, ^3J = 5.64 Hz), 7.47 (m, 6H), 7.46 (d, 4H, ^3J = 7.89 Hz), 7.25 (d, 4H, ^3J = 7.89 Hz), 2.27 (s, 6H, CH_3). $^{13}C\{^1H\}$ NMR (CD_3CN, 300 MHz): δ 157.0, 156.9, 155.2, 153.2, 152.1, 151.7, 140.7, 139.5, 138.0, 131.6, 129.5, 127.7, 127.6, 124.43, 124.40, 124.1, 118.2, 97.0 ($CC_{ethynyl}$), 83.5 ($CC_{ethynyl}$), 20.6 (CCH_3). FT-IR (KBr, cm^{-1}): υ 3439 (m), 2918 (m), 2219 (C≡C) (m), 2182 (C≡C) (s), 1619 (m), 1594 (s), 1462 (s), 1445 (s), 1314 (m), 1241 (m), 1106 (m), 836 (s), 769 (m), 725 (m), 556 (s). UV−vis (CH_3CN) λ, nm (ϵ, M^{-1} cm^{-1}): 440 (9700), 371 (55 700), 287 (68 800), 244 (38 400). FAB^+ (CH_3CN): 943.2 ($[M - PF_6]^+$). Anal. Calcd for $C_{48}H_{36}F_{12}N_6P_2Ru{\cdot}CH_3CN$: C, 53.20; H, 3.48; N, 8.69. Found: C, 52.95; H, 3.27; N, 8.49.

[Ruthenium(II)(2,2′-bipyridine)(5-{*p*-ethynyltoluene}-2,2′-bipyridine)$_2$](PF$_6$)$_2$ (3b). 3b was prepared according to general procedure 2 with 30 mg of **3** (0.03 mmol) in 2 mL of acetonitrile and 2 mL of benzene, 19.2 μL of *p*-ethynyltoluene (5 equiv, 0.15 mmol), 12.6 mg of [Pd(PPh_3)] (10% mol), and 1 mL of iPr$_2$NH. The crude product was purified by chromatography on a column packed with silica gel and eluting with an acetonitrile/water/aqueous saturated KNO_3 mixture (85:15:0 to 85:15:0.3). After anionic exchange, the analytically pure compound was obtained after recrystallization from dichloromethane/hexane (31 mg, 95%). ^1H NMR (CD_3CN, 300 MHz). FT-IR (KBr, cm^{-1}): υ 3444 (m), 2919 (m), 2219 (C≡C) (s), 2183 (C≡C) (m), 1619 (m), 1593 (s), 1509 (m), 1464 (s), 1436 (s), 1310 (m), 1239 (m), 837 (s), 764 (m), 730 (m), 557 (s). UV−vis (CH_3CN) λ, nm (ϵ, M^{-1} cm^{-1}): 468 (9800), 340 (66 700), 282 (39 200). FAB^+ (CH_3CN): 943.3 ($[M - PF_6]^+$), 798.2 ($[M - 2PF_6 + H]^+$). Anal. Calcd for $C_{48}H_{36}F_{12}N_6P_2Ru{\cdot}CH_3CN$: C, 53.20; H, 3.48; N, 8.69. Found: C, 53.09; H, 3.19; N, 8.54.

[Ruthenium(II)(5-{*p*-ethynyltoluene}-2,2′-bipyridine)$_3$](PF$_6$)$_2$ (4b). 4b was prepared according to general procedure 2 with 26 mg of **4** (0.0237 mmol) in 1.5 mL of acetonitrile and 1.5 mL of benzene, 15.5 μL of *p*-ethynyltoluene (5 equiv, 0.118 mmol), 10 mg of [Pd(PPh_3)] (10% mol), and 0.5 mL of iPr$_2$NH. The crude product was purified by chromatography on a column packed with silica gel and eluting with an acetonitrile/water/aqueous saturated KNO_3 mixture (85:15:0 to 85:15:0.2). After anionic exchange, the analytically pure compound was obtained after recrystallization from dichloromethane/hexane (26 mg, 94%). ^1H NMR (CD_3CN, 300 MHz): δ 8.50 (m, 6H), 8.11 (m, 2H), 8.08 (m, 4H), 7.80 (m, 6H), 7.41 (m, 3H), 7.38 (d, 6H, ^3J = 8.2 Hz), 7.23 (d, 6H, ^3J = 7.92 Hz), 2.28 (s, 9H, CH_3). $^{13}C\{^1H\}$ NMR (CD_3CN, 300 MHz): δ 156.5, 156.4, 155.7, 155.6, 153.39, 153.36, 153.1, 152.2, 152.01, 151.95, 140.6, 139.8, 138.1, 131.6, 129.5, 127.7, 127.8, 124.9, 124.8, 124.7, 124.2, 124.1, 123.9, 96.9 ($CC_{ethynyl}$), 96.8 ($CC_{ethynyl}$), 83.6 ($CC_{ethynyl}$), 83.5 ($CC_{ethynyl}$), 20.6 (CCH_3). FT-IR (KBr, cm^{-1}): υ 3368 (m), 2918 (m), 2872 (m), 2218 (m), (C≡C), 2183 (C≡C) (m), 1591 (s), 1509 (m), 1464 (s), 1437 (s), 1309 (m), 1238 (m), 1150 (m), 1083 (m), 837 (s), 785 (m), 729 (m), 557 (s). UV−vis (CH_3CN) λ, nm (ϵ, M^{-1} cm^{-1}): 468 (9800), 340 (66 700), 282 (39 200). FAB^+ (CH_3CN): 1057.2 ($[M - PF_6]^+$), 912.3 ($[M - PF_6 + H]^+$). Anal. Calcd for $C_{57}H_{41}F_{12}N_6P_2Ru{\cdot}CH_3CN$: C, 57.06; H, 3.57; N, 7.89. Found: C, 56.87; H, 3.47; N, 7.64.

5,5′-(1-Ethynylpyrene)-2,2′-bipyridine (L2). In a Schlenk flask, to a stirred degassed benzene (20 ml)/iPr$_2$NH(10 mL) solution of 5,5′-dibromo-2,2′-bipyridine (0.5 equiv, 77 mg, 0.24 mmol) were added sequentially [Pd(PPh_3)$_4$] (34 mg, 6% mol) and 1-ethynylpyrene (0.11 g, 0.49 mmol). The solution was heated overnight at 60 °C. After cooling, the yellow precipitate was filtered and washed with two portions of water (20 mL) and two portions of diethyl ether (10 mL). The analytically pure compound was recovered without any additional treatment (0.12 g, 82%). Due to its severe insolubility, the NMR spectroscopy was not applied for characterization. FAB^+ (M − NBA): 605.3 ($[M + H]^+$). Anal. Calcd for $C_{46}H_{24}N_2$: C, 91.37; H, 4.00; N, 4.63. Found: C, 91.02; H, 3.77; N, 3.69.

Photophysical Measurements. Absorption spectra were measured with a Hewlett-Packard 8453 diode array spectrophotometer or a Perkin-Elmer Lamda Uvikon 933 spectrophotometer. Static luminescence spectra were obtained with a single-photon counting spectrofluorimeter from Edinburgh Analytical Instruments (FL/FS 900). Excitation spectra were corrected with a photodiode mounted

Table 1. Photophysical Properties at Room Temperature and 77 K[a]

compound	$\lambda_{abs\ max}$[a] (nm)	ϵ ($M^{-1}\,cm^{-1}$)	$\lambda_{em\ max}$, 300 K (nm)	τ_{em}, TRPL[b] (μs)	τ, TA[c] (μs)	Φ_{em}[d]	$\lambda_{em\ max}$,[e] 77 K (nm)	τ_{em}, TRPL,[b] 77 K (μs)	ΔE_s[f] (cm^{-1})	k_r[g] ($\times 10^4\,s^{-1}$)	k_{nr}[g] ($\times 10^6\,s^{-1}$)
3	450	12100	616	0.84	0.77	0.0630	582	5.66	948	7.50	1.27
3a	420	54100	671	53.10	46.22	0.0110	670	110	22	0.02	0.02
3b	460	7530	640	1.51	1.10	0.0920	608	3.66	823	6.09	0.73
4	450	11900	611	0.50	0.51	0.0440	580	5.75	875	8.80	2.09
4a	420	70400	672	54.30	59.41	0.0086	671	110	22	0.02	0.02
4b	468	9800	634	1.38	1.29	0.1220	606	3.68	729	8.84	0.83
5	448	11040	636	1.26	1.10	0.0880	595	11.6	1084	6.98	0.87
5a	443	57700	690	4.86	5.00	0.0130	682	5.1, 10	170	0.26	0.21
5b	440	9800	675	0.72	0.69	0.0370	639	2.29	835	5.14	1.44

[a] Argon-saturated CH_3CN solutions unless otherwise noted. [b] Time-resolved photoluminescence (TRPL) lifetimes represent an average of at least five measurements and have an uncertainty of less than 10%. Here, the data were obtained using a 450 ± 2 nm excitation. Lifetimes were independent of monitoring wavelength throughout the emission envelope, except that of complex **5a** at 77 K. [c] Transient absorption decay lifetime measured with either 355 or 532 nm excitation. [d] Photoluminescence quantum yields were calculated using $[Ru(bpy)_3]^{2+}$ ($\Phi = 0.062$) in CH_3CN as the quantum counter, ±10%. [e] Emission spectra were taken at 77 K in 4:1 EtOH/MeOH with a 450 nm excitation. [f] Thermally induced Stokes shifts were calculated from the difference in $\lambda_{em\ max}$ at 300 and 77 K. [g] $k_r = \Phi_{em}/\tau_{em}$; $k_{nr} = 1/\tau_{em}(1 - \Phi_{em})$. It is assumed that the emitting excited state is produced with unit efficiency.

inside the fluorimeter that continuously measures the Xe lamp output. All fluorescence and luminescence experiments used optically dilute solutions (OD ~ 0.1) prepared in spectroscopic grade solvents. Radiative quantum yields (Φ_r) of each metal complex were measured relative to $[Ru(bpy)_3](PF_6)_2$, for which $\Phi_r = 0.062$ in deaerated CH_3CN which is accurate to 10%.[27] Frozen glass emission samples at 77 K were prepared by inserting a 5 mm (internal diameter) NMR tube containing a $10^{-5}-10^{-6}$ M solution (4:1 EtOH/MeOH) of the appropriate compound into a quartz-tipped finger dewar of liquid nitrogen.

Emission lifetimes were measured with a nitrogen-pumped broadband dye laser (2−3 nm fwhm) from PTI (GL-3300 N_2 laser, GL-301 dye laser), using an apparatus that has been previously described.[5,7] Coumarin 460 (440−480 nm) or BPBD (360−390 nm) was used to tune the unfocused excitation. Pulse energies were typically attenuated to ~100 μJ/pulse, measured with a Molectron Joulemeter (J4-05). Excited-state lifetimes were determined from the observed decays using fitting routines provided in Origin 6.1.

Nanosecond time-resolved absorption spectroscopy was performed using instrumentation that has been described previously.[5,7] Briefly, the excitation source was the unfocused second or third harmonic (532 or 355 nm, 5−7 ns fwhm) output of a Nd:YAG laser (Continuum Surelite I). Typical excitation energies were maintained near ~10 mJ/pulse. Samples were continuously purged with a stream of high-purity argon or nitrogen gas throughout the experiments. The data, consisting of a 10-shot average of both the signal and the baseline, were analyzed in Origin 6.1. All transient absorption measurements were conducted at the ambient temperature of 22 ± 2 °C.

Electrochemical studies employed cyclic voltammetry with a conventional three-electrode system using a BAS CV-50W voltammetric analyzer equipped with a Pt microdisk (2 mm^2) working electrode and a platinum-wire counter electrode. Ferrocene was used as an internal standard and was calibrated against a saturated calomel reference electrode (SCE) separated from the electrolysis cell by a glass frit presoaked with electrolyte solution. Solutions contained the electroactive substrate (ca. 3×10^{-3} M) in deoxygenated and anhydrous acetonitrile with tetra-*n*-butylammonium hexafluorophosphate (0.1 M) as the supporting electrolyte. The quoted half-wave potentials were reproducible within ±10 mV.

(27) Caspar, J. V.; Meyer, T. J. *J. Am. Chem. Soc.* **1983**, *105*, 5583−5590.

Results and Discussion

Prelude. The spectroscopic data of **3a** and **4a** in CH_3CN are quantitatively similar, demonstrating that the number of appended C≡C-pyrenyl units has no marked influence on the photophysical properties of these systems (Table 1). This simple result serves as an indicator for the lack of an excited-state equilibrium in these systems since the number density of pyrene chromophores would significantly influence the excited-state decay otherwise. For conciseness, comparisons throughout this paper will be made between **3a** and **5a** because both chromophores bear two C≡C-pyrenyl substituents. The photophysical behavior of these molecules will be contrasted to that of their corresponding ethynyltoluene structural model compounds (**3b** and **5b**) in the running text. Spectroscopic data obtained on the bromo-substituted synthetic precursors (**3**−**5**) and **4a** and **4b** are provided as Supporting Information. To facilitate direct comparisons, the spectroscopic and photophysical data obtained for all complexes investigated in this study are collected in Table 1.

Syntheses. Due to the pronounced insolubility of pyrene-substituted bpy ligands resulting from a weak dipole moment and the planarity of the molecules, the target complexes were difficult to synthesize according to classical procedures. We circumvented this problem through the preparation of the pivotal starting materials bearing unsubstituted bpy ligands (**1**) and 5-bromo-substituted (**2**) or 5,5′-dibromo-substituted (**3**) bpy ligands. Scheme 1 outlines the synthetic routes used for the generation of the metal complexes in this study. This strategy permitted the production of the ruthenium(II)−tris-(bpy) complexes **3**−**5** with varying numbers of reactive bromo functions. Quite interesting to note is that these complexes react smoothly under the Sonogashira−Hagihara cross-coupling conditions with 1-ethynylpyrene to provide the desired pyrene-substituted complexes (**3a**−**5a**) in very good yield (Scheme 1).[24,25] We note that there are many examples of this "chemistry on the complex" approach which permit the generation of desired products that otherwise would be rather prohibitive to synthesize.[24,25,28,29] The current protocol is convenient and versatile because of the mild conditions and the possibility of introducing various ethynyl-

Table 2. Electrochemical Properties at Room Temperature[a]

complex	E_{ap} or $E_{1/2}$ (V) [b] [ΔE_p (mV)]	E_{cp} or $E_{1/2}$ (V) [c] [ΔE_p (mV)]
3	1.36 (70)	−1.26 (irr), −1.52 (70), −1.76 (80)
3a	1.37 (irr)	−1.12 (74), −1.24 (78), −1.81 (irr)
3b	1.32 (70)	−1.17 (60), −1.32 (70), −1.65 (70)
4	1.39 (70)	−1.28 (irr), −1.52 (70), −1.76 (80)
4a	1.31 (irr)	−1.14,[d] −1.24,[d] −1.43,[d] −1.82[d]
4b	1.32 (60)	−1.14 (60), −1.28 (60), −1.45 (60)
5	1.36 (70)	−1.39 (irr), −1.52 (70), −1.77 (70)
5a	1.44 (irr)	−0.97 (70), −1.36 (80), −1.53 (70), −1.77 (70)
5b	1.31 (70)	−1.03 (60), −1.47 (60), −1.64 (80)

[a] Potentials determined by cyclic voltammetry in a 0.1 M $TBAPF_6$/CH_3CN solution, with a complex concentration of $\sim 3 \times 10^{-3}$ M. All potentials (±10 mV) are reported in volts vs SCE as the reference electrode, using Fc^+/Fc (+0.38 V, $\Delta E_p = 60$ mV) as the internal standard. Scan rate: 200 mV s^{-1}; $E_{1/2} = (E_{ap} - E_{cp})/2$ and $\Delta E_p = E_{ap} - E_{cp}$. [b] Ruthenium-based oxidation and radical cation of pyrene for the irreversible processes and ruthenium oxidation for the reversible processes. E_{ap} (anodic peak potential) corresponds to an irreversible electrode process (irr). [c] Ligand-based reduction, E_{cp} (cathodic peak potential) corresponds to an irreversible electrode process (irr). [d] Approximate values due to closely spaced redox processes.

grafted fragments, such as ethynyltoluene (**3b**−**5b**), which serve as important model compounds in the photophysical investigations. The uncoordinated free diimine ligands 5-pyrenylethynylene-2,2′-bipyridine (**L1**) and 5,5′-dipyrenylethynylene-2,2′-bipyridine (**L2**) were prepared independently to aid in spectroscopic assignments.

Electrochemistry. Table 2 presents the electrochemical data for all of the Ru(II) complexes at the heart of the present study. For the pyrene-grafted complexes, **3a**−**5a**, the first observed oxidation in cyclic voltammetry is metal-based and is irreversible on the electrochemical time scale. We believe that the close-lying pyrene oxidation process at slightly more positive potentials leads to the decomposition of each complex. In the absence of pyrene, these metal-based oxidations are reversible on the time scale of cyclic voltammetry. The ligand-based reduction processes are reversible, and a total of four sequential reduction processes can be resolved for complexes **4a** and **5a**. The easiest complex to reduce is **5a** (−0.97 V vs SCE), which is not surprising given the substantial degree of conjugation expected for the coordinated **L2** ligand. Since the first reduction processes in complexes **3a**−**5a** take place at potentials that are more positive than those of bpy, the LUMO in each case must reside on the ethynylpyrene-containing ligand(s). It can be inferred from the electrochemical data that the complex with the lowest expected energy gap, and therefore the lowest-energy electronic transitions, is **5a**, and this is confirmed below. The related *p*-ethynyltoluyl and bromo-substituted complexes display the

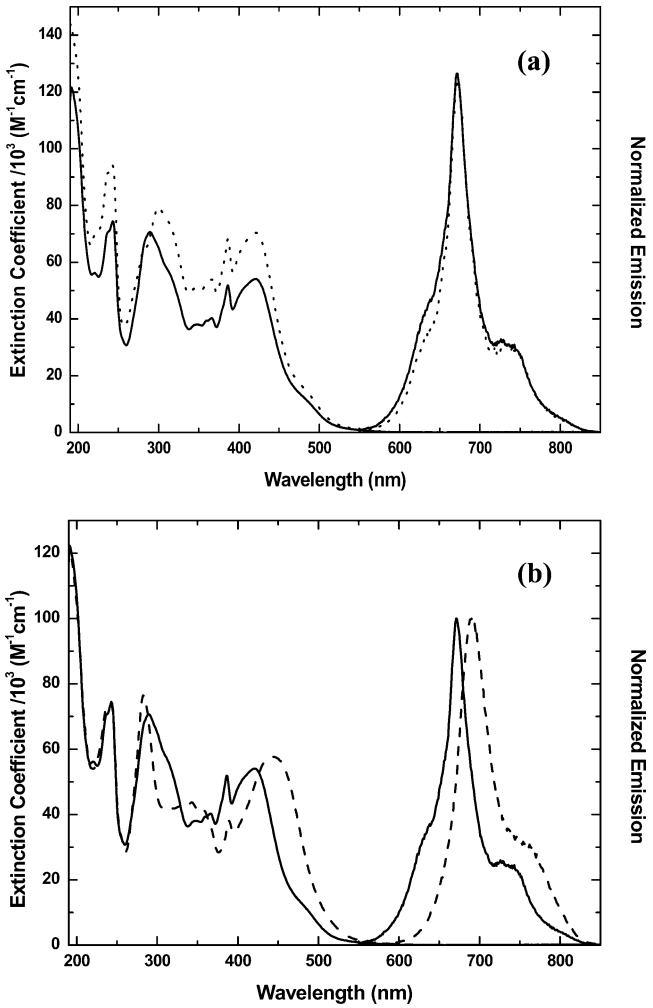

Figure 1. (a) Room temperature absorption and emission spectra of **3a** (——) and **4a** (·····) in degassed CH_3CN solution. (b) Room temperature absorption and emission spectra of **3a** (——) and **5a** (-----) in degassed CH_3CN solution. The emission spectra were measured with a 450 ± 2 nm excitation.

expected successive reductions of each bpy fragment. The potential range found for these waves reflects the σ-donating effect of the bromo groups versus the σ-withdrawing features of the ethynyl fragment, with the strongest effect being found when the two substituents are located on a single bpy ligand, such as in complexes **5**, **5a**, and **5b**.

UV−Visible Absorption. Figure 1 presents the UV−vis absorption and emission spectra obtained for **3a**−**5a** in CH_3CN. Table 1 lists the lowest-energy band maxima and the corresponding molar extinction coefficients. The electronic spectra of all other complexes are provided in the Supporting Information. The UV portion of the absorption spectra is dominated by ligand-localized $\pi-\pi^*$ transitions, whereas the visible portion of the spectra contains a combination of MLCT transitions, $d\pi(Ru) \rightarrow p^*(bpy)$ at higher energies and $d\pi(Ru) \rightarrow p^*(bipy(C{\equiv}C\text{-pyrene})_n)$ at lower energies. However, these MLCT transitions overlap the lowest-energy $\pi-\pi^*$-based transitions in ligands **L1** and **L2**. In the former case, this transition is observed as the sharp peak near 400 nm (Figure 1a). Figure 2 displays the UV−vis spectra obtained for the free ligands and **L2** in coordination equilibrium with Zn(II). Clearly, the pronounced $\pi-\pi^*$

(28) Pabst, G. R.; Pfuller, O. C.; Sauer, J. *Tetrahedron* **1999**, *55*, 8045−8064.
(29) Aspley, C. J.; Williams, J. A. G. *New J. Chem.* **2001**, *25*, 1136−1147.

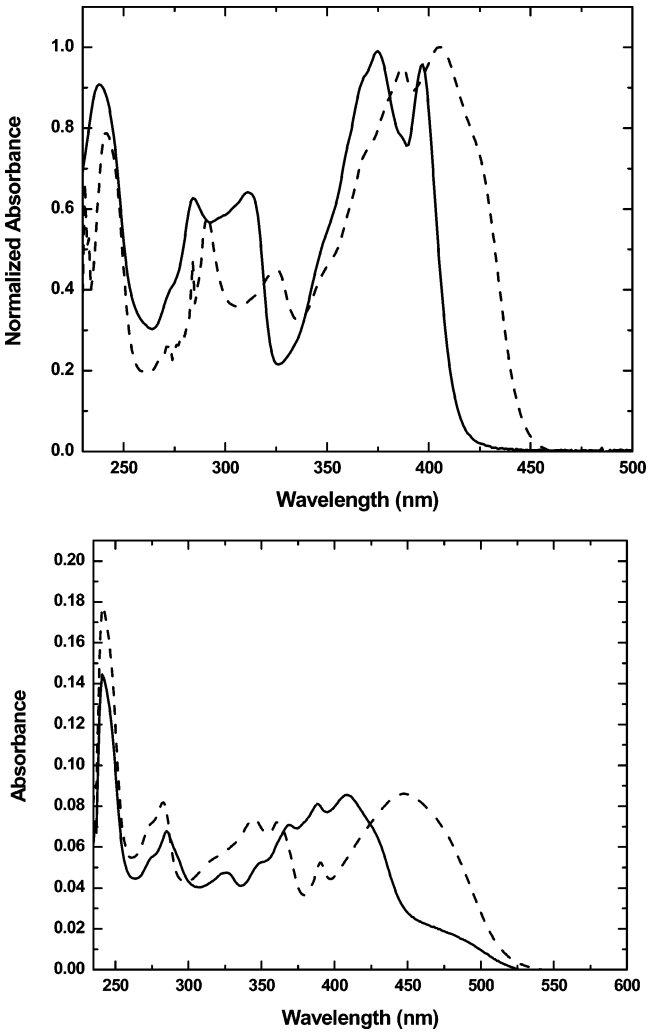

Figure 2. (Top) Normalized room temperature absorption spectra of **L1** (——) and **L2** (-----) in CH_3CN and THF, respectively. (Bottom) Room temperature absorption spectra of **L2** (——) and **L2** in the presence of zinc(II) acetate (-----) in chloroform.

transitions extend into visible wavelengths and are readily observed in the metal complexes (Figure 1). **L2** was mixed with Zn(II) to demonstrate that metal coordination planarizes the bpy ligand, rendering enhanced π-conjugation on the long axis of the ligand. Note that $CHCl_3$ was used to facilitate the dissolution of Zn(II) acetate. The net effect is a substantially red-shifted $\pi-\pi^*$ absorption band that now protrudes into the visible portion of the spectrum, substantially overlapping the low-energy MLCT transitions in **5a** (Figures 1 and 2). This concept is well-documented and has been applied to polymeric metal-ion sensory materials whose conjugation was improved upon metal binding to the bpy-containing fragments of the macromolecule.[30] In the present context of this paper, the position of the low-energy ground state $\pi-\pi^*$ absorption band of **L2** is crucial to the interpretation of the transient absorption data to be presented later.

Photoluminescence Properties. The photoluminescence characteristics of Ru(II)−diimine complexes possessing MLCT excited states are well-established and understood.[1,31−35] In general, room temperature Ru(II) MLCT-based emissions are characterized by broad and structureless emission bands, excited-state lifetimes on the order of hundreds of nanoseconds to ~1.5 μs, and corresponding radiative (k_r) and nonradiative (k_{nr}) rate constants near 10^5 and 10^6 s^{-1}, respectively. In addition, MLCT excited states display relatively large outer sphere reorganization energies (λ_s = 0.05−0.1 eV, ~400−800 cm^{-1}) that can be correlated to the thermally induced Stokes shift of the emission band (ΔE_s; recall that $\Delta E_s = 2\lambda_s$).[35,36] The six model systems containing either the Br (**3**−**5**) or the ethynyltoluene (**3b**−**5b**) units categorically display such characteristic MLCT emission behavior (see Table 1 and the Supporting Information).

In stark contrast, visible excitation leads to structured luminescence spectra in all of the C≡C pyrenyl-containing compounds, whose uncorrected maxima are 671 (**3a**), 672 (**4a**), and 690 nm (**5a**). The data obtained for all three complexes are displayed in Figure 1. In all of the cases, the excitation spectra completely superimpose the absorption spectra between 300 and 550 nm, indicating that internal conversion and intersystem crossing lead to a single low-energy emissive state (see the Supporting Information). While these structured emissions are significantly quenched by oxygen, the intensity of each spectrum diminishes symmetrically, supporting the notion that only one emissive state is present in these molecules.[13,14] We note that this does completely rule out potential contributions from coexisting excited states in thermal equilibrium or multiple excited states possessing similar excited-state properties. The photoluminescence quantum yields for **3a**−**5a** in deaerated CH_3CN that were measured relative to $[Ru(bpy)_3]^{2+}$ are 0.011, 0.009, and 0.013, respectively. The RT emission lifetimes of **3a**−**5a** measured in deaerated CH_3CN were 53.1, 54.3, and 4.86 μs, respectively. In all three cases, the values calculated for k_r and k_{nr} (Table 1) based upon these data are significantly smaller (by 1−3 orders of magnitude) than those observed in typical MLCT excited states. At the present time, we can only speculate on why the excited-state lifetimes measured in the 5-substituted molecules differ by a factor of 10 relative to those of the 5,5′-substituted complexes. One possibility is that the proximity of the ^{3}MLCT and ^{3}IL states in the latter is promoting some interaction between the states, rendering the photophysics somewhat between "pure" ^{3}MLCT and "pure" ^{3}IL characteristics.[16,17,20,23] More than likely, the lifetime difference simply reflects the true dynamic behavior of the phosphorescence of the system. Unfortunately, all attempts to measure room temperature phosphorescence of the free **L1** and **L2** ligands failed, even in the presence of external heavy atoms (ethyl iodide). Therefore, we had little choice but to rely on transient absorption spectroscopy to help shed some light on the lifetime

(30) Wang, B.; Wasielewski, M. R. *J. Am. Chem. Soc.* **1997**, *119*, 12−21.
(31) Meyer, T. J. *Prog. Inorg. Chem.* **1983**, *30*, 389−440.
(32) Meyer, T. J. *Acc. Chem. Res.* **1989**, *22*, 364.
(33) Crosby, G. A. *Acc. Chem. Res.* **1975**, *8*, 231−238.
(34) Juris, A.; Balzani, V.; Barigelletti, F.; Campagna, S.; Belser, P.; von Zelewsky, A. *Coord. Chem. Rev.* **1988**, *84*, 85.
(35) Chen, P.; Meyer, T. J. *Chem. Rev.* **1998**, *98*, 1439−1477.
(36) Whittle, C. E.; Weinstein, J. A.; George, M. W.; Schanze, K. S. *Inorg. Chem.* **2001**, *40*, 4053−4062.

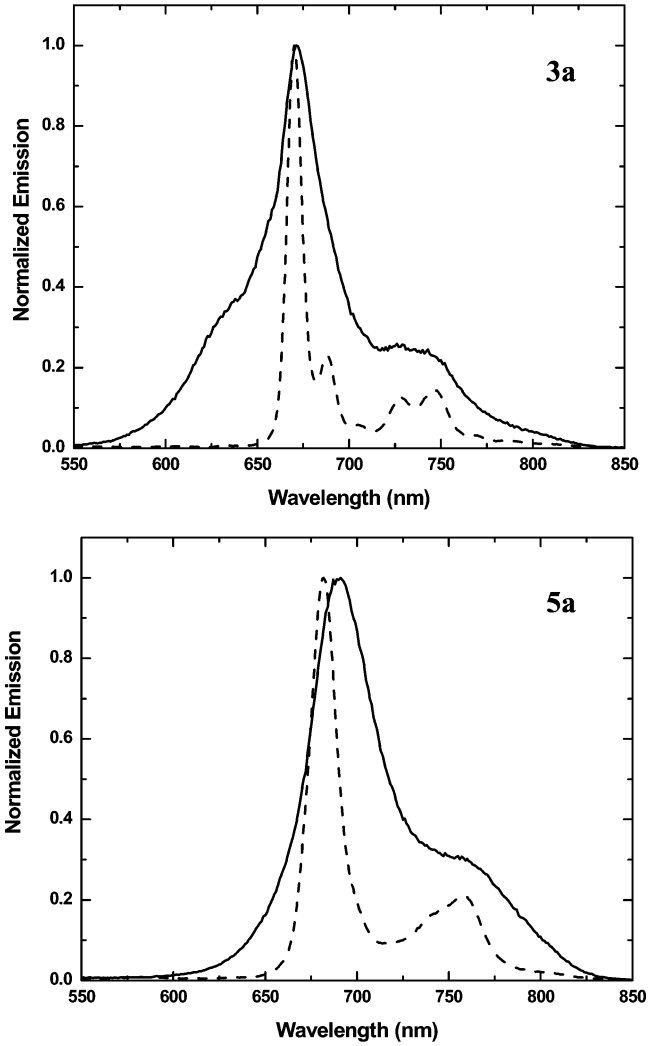

Figure 3. Emission spectra of **3a** and **5a** at RT (——) and 77 K (-----) in 4:1 EtOH/MeOH. The spectra were measured with a 450 ± 2 nm excitation.

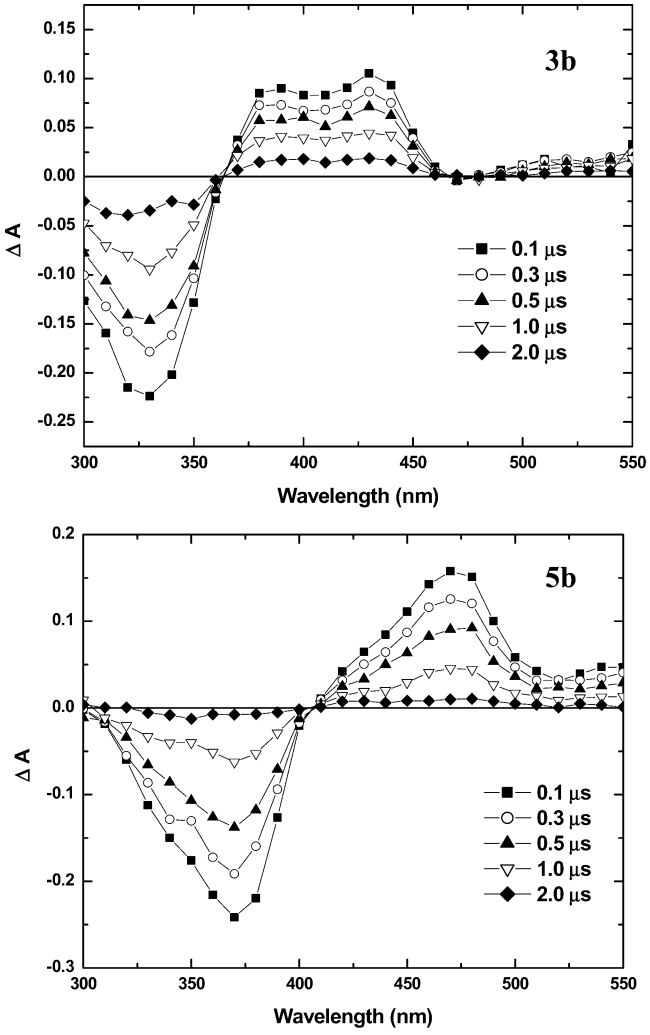

Figure 4. Excited-state absorption difference spectra of **3b** and **5b** in deaerated CH_3CN following a 532 nm pulsed-laser excitation. The delay times are specified on each spectrum.

observations and definitively assign one of the two possibilities mentioned above.

The emission spectra of **3a** and **5a** measured at 77 K in 4:1 EtOH/MeOH have maxima similar to those of their RT counterparts, with almost negligible thermally induced Stokes shifts of 45 and 170 cm^{-1}, respectively (Figure 3 and Table 1). The small values of ΔE_s indicate that the emissive states in these complexes are relatively nonpolar and not likely of MLCT origin. The 77 K spectra are narrower in shape but display similar vibronic progression relative to their RT spectra. **L1** and **L2** were strongly fluorescent at 77 K, and we were unsuccessful in observing any phosphorescence from these species. Every model system universally displayed 77 K spectra and excited-state lifetimes in a 4:1 ratio of EtOH/MeOH in accord with those expected for a lowest MLCT configuration (see Table 1 and the Supporting Information). All of the presented luminescence data for the pyrenyl-containing Ru(II) complexes are most consistent with a lowest excited state that is ^{3}IL in nature.

Transient Absorption Spectroscopy. Nanosecond laser-flash photolysis experiments also support the ^{3}IL emission assignment in **3a**−**5a**. Figure 4 presents the excited-state absorption difference spectra obtained for the ethynyltoluene-bearing model complexes **3b** and **5b** in deaerated CH_3CN following 532 nm excitation. This excitation wavelength ensures exclusive population of the MLCT manifold. Below 400 nm, the ligand $\pi-\pi^*$ ground-state transitions in **5b** are clearly bleached while there is a broad transient with a peak near 480 nm that extends past 550 nm into the region where the photoluminescence obscures our absorption difference spectra. We note that transients similar to those observed in our model compound **5b** have already been documented for $[Ru(bpy)_2(5,5'\text{-}C{\equiv}C\text{-phenyl-}2,2'\text{-bpy})]^{2+}$.[37] The unfamiliar appearance of these transients results from extremely large values for $\Delta\epsilon$ (large radical anion signal) throughout the visible spectra, which are so dominant that they completely obscure the MLCT ground-state bleaching signals in the visible spectra.[17,37] The difference spectrum of **3b** (and **4b**; see the Supporting Information) bears some resemblance to that obtained for **5b**, except the transient features are all blue-shifted. The bleach observed below 350 nm in **3b** is consistent with ground-state depletion of the $\pi-\pi^*$ absorption bands attributed to the 5-ethynylenetoluene-2,2′-bi-

(37) Wang, Y.; Liu, S.; Pinto, M. R.; Dattelbaum, D. M.; Schoonover, J. R.; Schanze, K. S. *J. Phys. Chem. A* **2001**, *105*, 11118−11127.

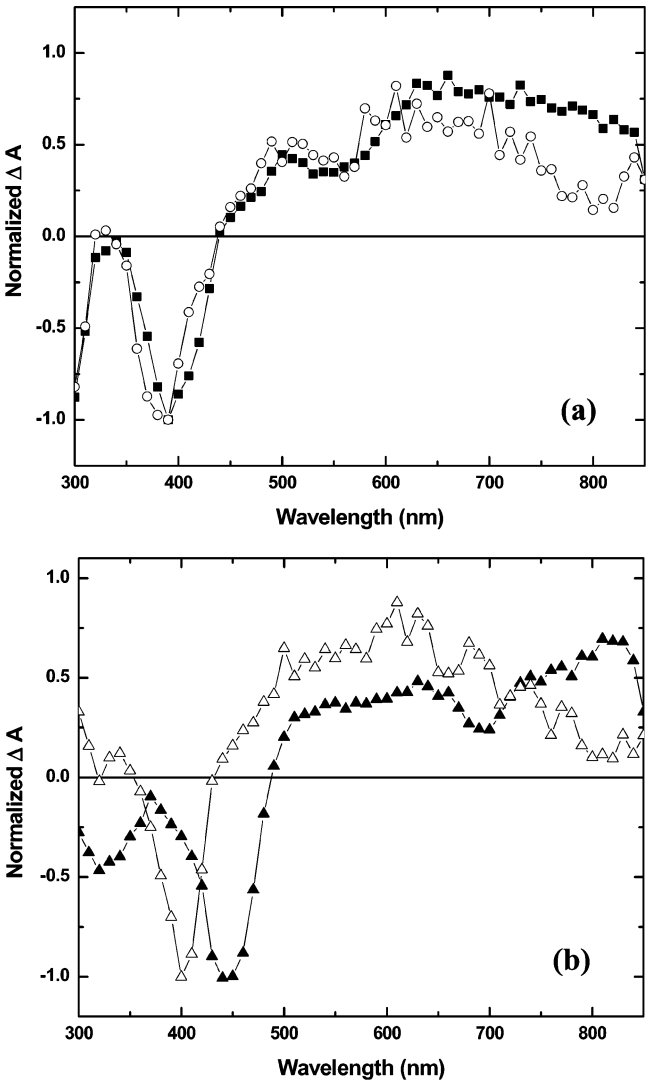

Figure 5. (a) Excited-state absorption difference spectra of **3a** (■) measured 4 μs after a 532 nm laser pulse along with the spectrum of **L1** (○) measured 8 μs after a 355 nm laser pulse in the presence of the triplet sensitizer thioxanthone. (b) Transient absorption difference spectra of **5a** (▲) in deaerated CH_3CN measured 1 μs after a 532 nm laser pulse and **L2** (△) in deaerated THF measured 8 μs after a 355 nm laser pulse in the presence of the triplet sensitizer thioxanthone.

pyridine moiety, and the absorption transients between 360 and 450 nm are believed to result from a radical anion signal possessing a high extinction coefficient. The blue shift of the transient spectrum in **3b** reflects the diminished conjugation of the ground-state absorption and radical anion signal relative to that observed in **5b**. These assignments can be further corroborated by the kinetic response of the absorption transients whose dynamics mirror those observed in each respective luminescence intensity decay within experimental error (Table 1). While this does not provide definitive proof of the nature of the states, the combination of all of the luminescence and absorption data suggests that the excited-state processes in **3b**−**5b** are most consistent with a MLCT configuration.

Figure 5a shows the excited-state difference spectra obtained for **3a** (delay = 4 μs) in CH_3CN following a 532 nm laser flash. This excitation wavelength was chosen to guarantee optical pumping of the MLCT manifold. We attempted to measure the transient absorption spectra of the free ligands **L1** and **L2**, but in both cases, the transients were weak. However, when we used the triplet sensitizer thioxanthone,[8,38] the intensity of both of these transients markedly increased. Also displayed in Figure 5a are the data obtained for **3a** and thioxanthone in CH_3CN (λ_{ex} = 355 nm), using a sufficient delay time (8 μs) for suppressing the thioxanthone sensitizer transients. In essence, the normalized spectra are nearly superimposed at all UV and visible wavelengths, illustrating that the lowest excited states in both **3a** and **L1** are of the same composition. On the basis that the excited-state spectrum of **L1** was easily triplet sensitized, displayed a lifetime of 45 μs in CH_3CN, and was extremely sensitive to dioxygen, the transient features are assigned to the ^{3}IL state of **L1**. In molecules **3a** and **4a**, there is little doubt that the lowest excited state is ^{3}IL-based and localized on **L1**.

Figure 5b displays the excited-state absorption difference spectrum obtained for **5a** in CH_3CN (λ_{ex} = 532 nm, delay time = 1 μs) and the triplet-sensitized spectrum of **L2** in MTHF (λ_{ex} = 355 nm, delay time = 8 μs). Of course, the 532-nm pump predominately accesses the low-energy MLCT transitions. The triplet-sensitized data measured for **L2** clearly represent the ^{3}IL excited state of the uncoordinated free ligand in solution, whereas the difference spectrum for **5a** is red-shifted in comparison. The lifetime of **L2** in MTHF is approximately 40−50 μs and cannot be measured more accurately due its highly insoluble nature. While the spectrum for **5a** is clearly distinct from that observed in the MLCT chromophore **5b** (Figure 4a), it also appears to be different from that of **L2**. A plausible explanation for this discrepancy results from the differences in conjugation lengths on the long axis of the bipyridine in the coordinated versus free-ligand structure. In essence, coordination of the 5,5′-ligand to the Ru(II) center planarizes the diimine structure, leading to the extended conjugation on the long axis with a concomitant red shift of the singlet $\pi-\pi^*$ absorption transitions and the observed room temperature phosphorescence. As a result, transient absorption measurements obtained using free 5,5′-dipyrenylethynylene-2,2′-bipyridine (**L2**) are blue-shifted relative to those of its Ru(II) complex (**5a**), particularly noticeable in the relative wavelengths of the $\pi-\pi^*$ ground-state bleaching and also consistent with the ground-state absorption shifts measured upon Zn(II) coordination to **L2** (Figure 2). Unfortunately, all attempts to perform transient absorption measurements on the Zn(II) chelate of **L2** in $CHCl_3$ were inconclusive due to rapid sample decomposition during the course of the experiments. Although the discrepancy in the excited-state lifetime between free **L2** and **5a** may cause alarm, it is not surprising that the partially conjugated **L2** exhibits photophysical behavior similar to that of free **L1**. Although we cannot completely rule out some type of electronic interaction between the MLCT and ^{3}IL states in **5a**, it would be surprising if this compound's excited-state behavior is significantly different from that of **3a** or **4a**. This is especially true given the structural and energetic similarities exhibited

(38) Rogers, J. E.; Kelly, L. A. *J. Am. Chem. Soc.* **1999**, *121*, 3854−3861.

by all three molecules. We conclude that other than the differences in the excited-state lifetimes, there is no marked compelling evidence for any interactions between multiple, close-lying excited states in these molecules, and that the RT phosphorescence emanates from the lowest ^{3}IL state, localized on **L1** or **L2** in each case.

Conclusion

A new synthetic protocol for the preparation of Ru(II)−bipyridine complexes bearing multiple appended ethynyl-pyrenyl or *p*-ethynyltoluyl fragments has been presented. In cases where two or three pyrenyl modules are present in the diimine ligand structures, extended RT excited-state lifetimes in deaerated solution were observed. In all of the cases, it appears that the lowest excited states are ^{3}IL in character, displaying RT phosphorescence. While the data presented for **3a** and **4a** are consistent with relatively pure ^{3}IL-based phosphorescence emerging from the pyrenyl-containing diimine ligand(s), the behavior of **5a** is somewhat distinct. Although we cannot definitively rule out potential electronic interactions in **5a**, we believe its photophysics is simply an inherent property of the conjugated ligand system of **L2**. The current work illustrates that with appropriately substituted ligands, Ru(II) MLCT complexes can generate long-lived phosphorescence at RT, which is quite rare. Such molecules are of fundamental interest yet are also poised for potential applications in optoelectronics and luminescence-based technologies.

Acknowledgment. The Bowling Green State University (BGSU) portion of the work was supported by the National Science Foundation (CAREER Awards CHE-0134782 and CHE-0234796) and the ACS (ACS-PRF 36156-G6). D.S.T. and D.V.K. were supported by McMaster Fellowships from BGSU. The work performed at the ECPM/ULP was supported by IST/ILO EC Contract 2001-33057 and the Centre National de la Recherche Scientifique. Transient absorption measurements were performed in the Ohio Laboratory for Kinetic Spectrometry at BGSU.

Supporting Information Available: Additional static and dynamic spectroscopic data. This material is available free of charge via the Internet at http://pubs.acs.org.

IC049288+